Expression , Purification, and Characterization of the Recombinant, Two-component, Response Regulator ArlR From Fusobacterium Nucleatum

Ruochen Fan (fanruochen@mail.dlut.edu.cn)
Dalian University of Technology; Dalian Minzu University
Zhuting Li
Dalian Minzu University: Dalian Nationalities University
Chunshan Quan
Dalian Minzu University: Dalian Nationalities University
Lulu Wang
Dalian University of Technology; Dalian Minzu University
Xian Shi
Dalian Minzu University: Dalian Nationalities University
Xuqiang Zhang
Dalian Minzu University: Dalian Nationalities University
Yuesheng Dong
Dalian University of Technology

Research Article

Keywords: two-component system, Fusobacterium nucleatum, protein expression and purification, protein interaction

Posted Date: June 7th, 2021

DOI: https://doi.org/10.21203/rs.3.rs-571272/v1

Version of Record: A version of this preprint was published at Applied Biochemistry and Biotechnology on January 14th, 2022. See the published version at https://doi.org/10.1007/s12010-021-03785-5.

Abstract

Fusobacterium nucleatum is associated with the incidence and development of multiple diseases, such as periodontitis and colorectal cancer (CRC). Till now, studies have proved only a few proteins to be associated with such pathogenic diseases. The two-component system is one of the most prevalent forms of bacterial signal transduction related to intestinal diseases. Here we report a novel, recombinant, two-component, response-regulator protein ArlR from the genome of *F. nucleatum* strain ATCC 25586. We optimized the expression and purification conditions of ArlR; in addition, we characterized the interaction of this response regulator protein to the corresponding histidine kinase and DNA sequence. The full-length ArlR was successfully expressed in six of the *E. coli* host strains. However, optimum expression conditions of ArlR were present only in *E. coli* strain BL21 Condon plus (DE3) RIL that was later induced with isopropyl β-D-1-thiogalactopyranoside (IPTG) for 8 h at 25 °C. The SDS-PAGE analysis revealed the molecular weight of the recombinant protein as 27.3 kDa and approximately 90% purity after gel filtration chromatography. ArlR was biologically active after its purification. Therefore, it accepted the corresponding phosphorylated histidine-kinase phosphate group and bound to the analogous DNA sequence. The binding constant between ArlR and the corresponding histidine kinase is 1.28 μM, while the binding constant between ArlR and the bound DNA sequence is 37.5 μM. Altogether, these results illustrate an effective expression and purification method for the novel two-component system protein ArlR.

Introduction

Fusobacterium nucleatum is a typical, opportunistic, and pathogenic gram-negative bacteria related to the incidence and development of diseases such as periodontitis, head and neck cancer, poor pregnancy, and colorectal cancer (CRC) [1-4]. *F. nucleatum* can invade endothelial cells and adhere to several mammalian cells, including murine lymphocytes and macrophages, and human oral epithelial cells to participate in colonization and evade host defenses [5, 6]. Noticeably, *F. nucleatum* has been reported to be present in a high abundance in CRC cells [7]. Many studies have shown that *F. nucleatum* plays a significant role in increasing the proliferation and migration of CRC cells; because of it forming a pro-inflammatory micro-environment suitable for the development of CRC and enhancing the drug resistance of CRC cells [8-10]. In dental biofilms, *F. nucleatum* through periodontitis-pathogen accretion connects the early colonizing commensals and late pathogenic colonizers. Also, *F. nucleatum* functions as a connector between the primary and secondary colonizing organisms. Therefore, *F. nucleatum* is commonly known as a "bridge organism" [11, 12].

A two-component system (TCS) is a form of signal-transduction system that mainly exists in microorganisms and plants [13]. Bacterial signal-transduction systems mainly consist of two proteins: histidine-kinase and transcription protein. Bacterial signal-transduction systems use kinases with extracellular or periplasmic sensing domains for transferring the phosphate groups to its corresponding response regulator protein; thus, altering the levels of gene expression [14-21]. TCSs are involved in bacterial pathogenicity, biofilm formation, and physiological responses to osmotic changes in various

bacteria [14]. Recently, many studies have found that the TCS is related to intestinal diseases [22-28]. Wakimoto S. et al. (2013) proved that phosphate regulon transcriptional regulatory protein (PhoB) was necessary for *Bacteroides fragilis* survival in peritoneal abscesses [26]. Likewise, Massmig M. et al. (2020) suggested that the CntAB two-component system in the gut micobiome catalyzes the oxidative cleavage of L-carnitine into TMA related to cardiovascular diseases [23]. Another significant characteristic of the two-component system is its ability to promote colonization of bacteria in the mammalian intestine; for example, FusKR TCS is required for the robust colonization of enterohemorrhagic *E. coli* in the mammalian intestine [29]. The CpxRA TCS of *Salmonella enterica* plays a significant role in gut colonization in *Salmonella*-induced colitis [30]. Moreover, the two-component system also affects the metabolic response of the intestinal bacteria [31-33]. Sonnenburg ED. et al. (2006) demonstrated that hybrid TCSBT3172 functions as a metabolic reaction center by coupling the nutrient-sensing to the dynamic regulation of monosaccharide metabolism [32], and Liu M. et al. (2019) proved that CitAB TCS in *Vibrio cholerae* contributes to the anaerobic citrate fermentation [31].

TCSs are potential targets for antimicrobial drug design. Since the histidine phosphorylation of TCS in bacteria differs from serine/tyrosine/threonine phosphorylation of signaling systems in mammalian cells, TCS inhibitors may exert less toxicity in the host [34, 35]. TCSs have been well-studied in several pathogenic bacteria such as *Escherichia coli* and *Pseudomonas aeruginosa*; however, they have not been well-studied in *F. nucleatum*. In this study, we have analyzed the two-component system of *F. nucleatum* ATCC 25586, one of the recently sequenced genome strains, which further enhances our knowledge and understanding of its physiological function and pathogenic mechanism of virulence.

In summary, this study provides a method for the expression, purification, and characterization of the response regulator (RR), TCS protein ArlR. This paper is the first to report the purification and characterization of the TCS-RR protein ArlR in *F. nucleatum*.

Methods

Bacterial strains, plasmids, enzymes, and chemicals

We purchased *F. nucleatum* strain ATCC 25586 from American Type Culture Collection (ATCC). The *E. coli* strains (DH5α, BL21 (DE3), BL21-Condon Plus (DE3) RIL, BL21 (DE3) pLysS, Tuner (DE3), C43 (DE3), Transetta (DE3)), and the plasmid *pET-28a* were in the preserved state in our laboratory. Also, we purchased the HS DNA polymerase and restriction enzyme from Takara BioEngineering (Dalian, China). DNA gel extraction and plasmid purification kits were purchased from Axygen (corning, America). Chemicals used, such as kanamycin, chloramphenicol, and β-D-1-thiogalactopyranoside (IPTG), were of analytical grade unless otherwise stated.

Bioinformatics Analysis

The complete genome sequence of *F. nucleatum* ATCC 25586 (*NP_603483.1*) was obtained in FASTA format from the NCBI database (https://www.ncbi.nlm.nih.gov/). The Stockholm format files from the

conserved protein domain family HATPase_c (Pfam02518) of histidine-kinase (HK) and from the conserved domain family Response_reg (Pfam00072) of RR protein was downloaded from the Pfam database (http://pfam.xfam.org/). In HMMER 2.0 software, the command hmmbuild (see Table 1 for commands) was used to construct the hidden Markov models for HATPase_c and Response_reg, which finds out the HKs and RRs with HATPase_c and Response_reg domains. Subsequently, comparing the obtained results with those on the MiST website provides a comprehensive classification of the signal-transduction systems [36]. Finally, we stated three points to determine a pair of two-component signal systems: 1) histidine kinase catalytic domain HATPase_c must be located at the HK C-terminus; 2) the upstream of HATPase_c should have the phosphate receptor domain HisKA; 3) N-terminus of RR should be the phosphate receptor in the target TCSs. Multiple sequence alignments were performed using ClustalX and ESPript [37]. The molecular architecture of the TCS response regulator proteins and ArlR was determined by SMART and Pfam [38]. The structure was predicted from Phyre^2 [39].

Construction of the recombinant plasmid

Using the restriction-free (RF) cloning method, we constructed the *pET-28a -arlR* plasmid. The RF-cloning.org web server was used to design primers F1 ($^{5'-}$ CAGCCATCATCATCATCATCACAGCAGC *ATGTTATTATTTTCTTGGGTGAGG* $^{-3'}$, where the sequence in italics represents *arlR* gene-specific region) and R1 ($^{5'-}$ GGAGCTCGAATTCGGATCCGCG *TTAATCCTCTTTATATTGAAATATATAG* $^{-3'}$, where sequence in italics represent the *arlR* gene-specific region) complementary to insert and vector [40]. The *arlR*-megaprimers (the first polymerase chain reaction (PCR)) were amplified by PCR, using the primers F1 and R1 from the genomic DNA of strain ATCC 25586 of *F. nucleatum*. The PCR product was collected by the Axygen Prep DNA Gel Extraction Kit and then inserted into *pET-28a* plasmid by the secondary PCR reaction (100 ng megaprimers, 200 μM dNTP, 25 ng *pET-28a* vector, and 1 U HS DNA Polymerase). The collected PCR product was treated with 20 U DpnI and then transformed into the *E. coli* strain DH 5α using electroporation.

The cytoplasmic domain of histidine kinase (a*rlSC*) was amplified with the primers F2 ($^{5'-}$ CAGCCATCATCATCATCATCACAGCAGC *GATAAATTTAAAAATTCACTTG* $^{-3'}$, where sequence in italics represents *arlSC* gene-specific region) and R2 ($^{5'-}$ GGAGCTCGAATTCGGATCCGCG *TTAAAATAGTAGTGTTATTTTTGTTCCC* $^{-3'}$, where sequence in italics represents *arlSC* gene-specific region). The cloning steps of a*rlSC* were carried out as described above for ArlR.

Expression of the recombinant ArlR

Six different *E. coli* host strains (BL21 (DE3), BL21-Condon plus (DE3) RIL, BL21 (DE3) pLysS, Tuner (DE3), C43 (DE3), Transetta (DE3)) were used to express ArlR. We selected a positive transformant from each of the host strains and cultured it overnight at 37 °C in 20 mL Luria-Bertani (LB) medium supplemented with the corresponding antibiotics; next, the liquid culture medium was transformed into 50 mL LB medium with 1% culture inoculation and cultivated at 37 °C until the OD_{600} reached 0.6 – 0.8. Subsequently, the protein expression was induced by the addition of 0.5 mM IPTG at different intervals of

time (8 h, 20 h) and temperatures (16 °C, 25 °C). The cells were harvested by centrifugation, resuspended in 1 mL buffer A (20 mM Tris-HCl pH 8.0, 150 mM NaCl), and disrupted by sonication for 5 min on ice. The lysate was then centrifuged at 18,200 × g for 10 min at 4 °C. The soluble and insoluble proteins were detected by sodium dodecyl sulfate-polyacrylamide gel electrophoresis (SDS-PAGE).

Purification of the recombinant protein

The *E. coli* host strain with the highest protein expression was selected for large-scale protein expression through the subsequent purification steps. Five grams of wet cells, harvested by centrifugation, were resuspended in 35 mL of buffer A. Aliquots of 1 mL were taken from the 35 mL resuspended buffer. Each aliquot was centrifuged for precipitation. Cells were resuspended in buffer A containing different additives (5% glycerol, 50 mM L-Arg, 50 mM betaine, 1% Triton X-100, 50 mM L-Arg and 50 mM L-Glu) separately and, respectively. The cells were then disrupted by sonication and analyzed by 15% SDS-PAGE, which revealed buffer A with 5% glycerol to be the most suitable buffer. The crude extracts were precipitated by centrifugation at 18,200 × g for 45 min at 4 °C. The soluble supernatant of the lysate was mixed with 5 mL Ni-NTA affinity resin (GE Healthcare, USA), and the solution was incubated for 30 min in a rotating shaker at 4 °C. We further loaded the resulting slurry onto a 50 mL column, where the resin was washed away with buffer B (20 mM Tris-HCl, pH 8.0, 150 mM NaCl, 5% glycerol, 20 mM imidazole). The target protein was eluted from the column by buffer C (20 mM Tris-HCl, pH 8.0, 150 mM NaCl, 5% glycerol, 250 mM imidazole). The eluted protein was concentrated and loaded onto the HiLoad Superdex 200 26/60 column (GE Healthcare, USA) and was equilibrated with buffer A containing 5% glycerol. We used 15% SDS-PAGE and Coomassie staining to analyze the samples obtained from each purification step. The expression and purification of ArlSC were carried out as described above for ArlR.

Circular dichroism spectroscopy

Circular dichroism (CD) spectroscopy was performed on a Chirascan^{TM} spectrometer (Applied Photophysics Ltd) with a 0.1 cm path length of the quartz cuvette. The samples were prepared using buffer A (20 mM Tris-HCl, pH 8.0, 150 mM NaCl) and 0.2 mg/mL ArlR. The sample was 200 µL with 1 nm bandwidth length, 185 – 260 nm scanning range, and 0.5 s time-per-point. The spectrum of the target protein at 191 – 260 nm was obtained over a range of temperatures starting from 20 °C and incrementally increasing to 94 °C, which we used to measure the ArlR melting temperature (Tm). Ultimately, the Tm value was calculated by the Global 3 software, while the secondary structure was visualized and analyzed using the Deconvolution software that comes with the instrument.

Autophosphorylation and phosphoryl transfer assays

Purified ArlSC was pre-equilibrated with the phosphorylation buffer (20 mM Tris-HCl at pH 8.0, 50 mM KCl, 5 mM $MgCl_2$) in a final volume of 100 µL. Subsequently, an autophosphorylation reaction was initiated by adding the aliquots of ATP to a final concentration of 10 µM and lasting for 30 min at 25 °C. The intrinsic kinase activity of ArlSC was measured using the Promega Kinase-Glo Luminescent Kinase Assay Kit. As for the phosphoryl transfer assays, the purified ArlR was added to the phosphorylated ArlSC

to initiate phosphotransfer reaction in the phosphorylation buffer with 10 μM ATP for 10 min at 25 °C. Lastly, the persistent ATP was measured by the Promega Kinase-Glo Luminescent Kit.

Microscale thermophoresis (MST) assay

As previously reported [41], the affinity of ArlR and ArlSC was determined by MST using Monolith NT.115 (NanoTemper Technologies, Germany). Briefly, ArlSC was labeled with NHS fluorescent dye and centrifuged at 18,200 ´ g for 10 min to eliminate precipitation. A 16 step 1:1 (v/v) ArlR serial stock, with twofold dilution, was prepared with the MST buffer (50 mM Tris-HCl, pH 8.0, 150 mM NaCl, 10 mM $MgCl_2$, 0.05% Tween-20), such that each dilution step reduced the protein concentration by 50%. Equal volumes of the labeled ArlSC and unlabeled ArlR were mixed, incubated for 5 min at room temperature, and added to capillaries for measurement. The data were analyzed using NanoTemper Analysis software.

According to the protocol as described previously [42], the binding of ArlR to its promoter was determined by MST using Monolith NT.115 (NanoTemper Technologies, Germany).Briefly, the promoter of ArlR was amplified with primers of F2 ($^{Cy5-5'-}$ CCTCACCCAAGAAAATAATAATAAC $^{-3'}$) and R2 ($^{5'-}$ CCAAATAAGGCATAAGAGAGC $^{-3'}$). A 16 step 1:1 (v/v) serial ArlR stock, with twofold dilution, was prepared with the MST buffer (50 mM Tris-HCl at pH 8.0, 150 mM NaCl, 10 mM MgCl2, 0.05% Tween-20). Equal volumes of the labeled DNA and unlabeled protein solutions were mixed and incubated for 5 min at room temperature. Lastly, the samples were loaded into silica capillaries and measured by MST instrument.

Results

Two-component system in F. nucleatum strain ATCC 25586

The two-component system of *F. nucleatum* strain ATCC 25586 was searched by the software HMMER, and compare with the results on the website MiST. Four pairs of the typical TCSs identified were CzcRS, ArlRS, LytRS, and YesNM, respectively. The response regulator (RR) proteins in *F. nucleatum* strain ATCC 25586 contained a conserved receiver domain and a variable effector domain (Fig. 1a). Previous studies have reported that the response regulatory ArlR contributes to adhesion, autolysis, and multidrug resistance [43, 44]. The alignment analysis between the ArlR in *F. nucleatum* ATCC 25586 and other reported response regulation ArlR showed a high sequence similarity. By comparing with the sequence of the ArlR protein in *Staphylococcus aureus*, it can be said that the conserved aspartate phosphate group receptor in the 61st residue is most likely the phosphate acceptor site (Fig. 1d). These results indicated ArlR protein in *F. nucleatum* strain ATCC 25586 as a typical response regulatory protein in the two-component system.

ArlR is a member of the OmpR/PhoB superfamily that consists of a receiver domain and an effector domain. However, the domain predicted from Pfam (Fig. 1b) and the structure predicted from the Phyre^2 (Fig. 1c) shows an extended flexible region between these two domains. Also, the gene of the ArlR is composed of a large amount of AT base pairs. Therefore, we predict that these conditions may cause

certain difficulties in the expression or purification of ArlR, so we optimized its expression and purification conditions.

Expression and purification of the recombinant ArlR

The *arlR* gene from *F. nucleatum* strain ATCC 25586 was inserted into the *pET-28a* plasmid to create a recombinant plasmid and then separately transformed into the six different host strains. The expression of ArlR protein varied significantly with the varying host strains after inducing 0.5 mM IPTG for 8 h or 20 h, at 16 °C or 25 °C. Host strains had the most significant impact on ArlR expression; however, the best expression conditions were present in *E. coli* host strain BL21 Condon plus (DE3) RIL induced with 0.5 mM IPTG for 8 h at 25 °C (Fig. 2a). Several additives such as glycerin, L-arginine, 50 mM L-Arg and 50 mM L-Glu, betaine, 1% Triton X-100 were added to increase purified ArlR soluble protein. SDS-PAGE revealed that the recombinant ArlR was expressed both in the soluble and inclusion body forms; and the solubility of ArlR could increase slightly by adding 5% glycerol to the additive (Fig. 2b).

Further, ArlR was purified by Ni-NTA affinity chromatography and gel filtration chromatography. Using Ni-NTA affinity chromatography, we obtained ArlR with a high concentration and purity (Fig. 3a). However, using the purification process of the gel filtration chromatography, the ArlR protein got slightly degraded (Fig. 3b). ArlR was collected into a 50-mL concentration tube after gel filtration chromatography and was concentrated to 500 µL by centrifugation at 4 °C. The yield of ArlR was about 10 mg/L of culture solution. The secondary structure and thermal stability of the purified ArlR were further determined by circular dichroism spectroscopy. Two minimum peaks at 208 nm and 222 nm of ArlR are the characteristic structural peaks of α-helix; thus, indicating that the purified ArlR has secondary structure-activity (Fig. 3c). Moreover, circular dichroism (CD) spectra of ArlR at temperatures 20 °C – 94 °C showed the changes in the secondary structure of the protein at different temperatures (Fig. 3d). Consequently, the height of the characteristic peak of the ArlR α-helix gradually decreased with the increase in temperature, which may be due to the dissociation and the changes of the protein secondary structure. Calculations show the Tm of ArlR as 55.8 °C.

The phosphotransferase activity of the phosphorylated ArlSC to ArlR

Kinase-Glo™ Luminescent Kinase assay detected the presence of the kinase activity of cytoplasmic domain of histidine kinase (ArlSC). As shown in Fig. 4a, the luminescence intensity of the reaction system gradually decreased, that is, the remaining ATP content in the kinase buffer gradually decreased with the increase in the concentration of ArlSC; thus, suggesting that the ArlSC protein has histidine kinase activity. Using microscale thermophoresis (MST) experiment, we investigated an interaction between the phosphorylated histidine-kinase cytoplasmic domain (P-ArlSC) and its corresponding response regulator (ArlR). The outcome reveals that P-ArlSC can interact with ArlR, with high affinity (Kd = 1.28 µM, Fig. 5a). We further investigated the phosphotransferase activity of P-ArlSC to ArlR by adding the different concentrations of ArlR to the P-ArlSC (3 µM) solution containing ATP. The remaining ATP content in the kinase buffer gradually decreased with an increase in the concentration of ArlR; thus, suggesting that the P-ArlSC protein has the phosphotransferase activity to ArlR (Fig. 4b).

The binding of phosphorylated ArlR to its promoter

The response regulatory protein of the TCS can usually be in combination with its promoter to regulate its expression. To test this hypothesis, we designed a pair of primers labeled with cy-5 and amplified approximately 300 bp sequence present between the *arlR* gene (*Fn1260*) and its upstream gene (*Fn1259*) in *F. nucleatum* strain ATCC 25586*.* Using MST experiment, we confirmed the interaction between P-ArlR and the corresponding DNA sequence. The intermolecular Kd value of P-ArlR and its promoter is 37.5 μM (Fig. 5b).

Discussion

The ArlR is a member of the OmpR/PhoB subfamily, the largest subfamily of bacterial RRs [45]. These RRs can bind to DNA; thus, activating transcription. The TCS of ArlRS plays a significant role in gram-positive bacteria, such as *Staphylococcus aureus* and *Staphylococcus epidermidis*. Bai J et al. (2019) confirmed that eliminating the ArlRS TCS in certain strains of *Staphylococcus aureus* may increase sensitivity to oxacillin [46]. Moreover, JN Radin et al. (2016) proved that the ArlRS TCS enhanced the proliferation of *Staphylococcus aureus* in the presence of calprotectin-induced manganese-starvation [47] . However, what is the function of the TCS of ArlRS in gram-negative bacteria is still unclear. We found that the ArlRS TCS of *F. nucleatum* is highly homologous to the ArlR TCS of *Staphylococcus aureus*. The ArlR was expressed and purified in vitro to investigate the function of ArlRS from *F. nucleatum*. Results found that ArlR is a typical RR protein which could receive a phosphoryl group from its corresponding histidine-kinase cytoplasmic ArlSC through phosphoryl transfer. Therefore, this result suggests that the interaction between ArlS histidine-kinase and ArlR response regulator protein mainly relies on the cytoplasmic domain of histidine-kinase, while the transmembrane-domain of ArlS histidine-kinase may play significant roles in the sensing and transmitting of signals.

Studies have reported that different host strains of *E. coli* have different characteristics. Therefore, different host strains may be used to express different types of proteins [48, 49]. We proposed six host strains of *E. coli* to explore the differences in the expression of the same protein in different host bacteria. The results showed that the highest expression of ArlR was in *E. coli* BL21-Condon plus (DE3) RIL host strain. The genotype of E. coli BL21-Condon plus (DE3) RIL is derived from E. coli BL21 (DE3) and possesses rare tRNAs for expressing AT-rich genomes [49]. The genome sequence of *F. nucleatum* strain ATCC 25586 had 73% more AT base [50] , and the AT content of the *arlR* gene in the strain was 74.3%. Therefore, we suggest a preferential selection of *E. coli* BL21-Condon plus (DE3) RIL host strain during the expression of proteins in *F. nucleatum*. During protein purification, the purpose of adding 5% glycerol to the buffer is that besides increasing the solubility of ArlR protein, it can effectively prevent protein degradation. In addition, we recommend using a smaller gel filtration column and a faster flow rate, which can significantly reduce the degradation and improve the purity of ArlR.

Conclusion

Altogether, we identified four groups of TCS in *F. nucleatum* strain ATCC 25586 and successfully cloned the *arlR* gene into *pET-28a* by restriction-free (RF) cloning method. We obtained ArlR with a purity greater than 90% and concentration above 15 mg/mL by using the optimized expression and purification conditions. In addition we proved that the purified ArlR RR protein could receive phosphoryl group from its corresponding HK cytoplasmic ArlSC, and the phosphorylated ArlR could binds to its promoter. These results also suggest that one should preferentially select *E. coli* strain BL21-Condon plus (DE3) RIL as the host bacteria during the expression of proteins from *Fusobacterium nucleatum.*

Declarations

Funding

This work was supported by the National Natural Science Foundation of China (Grant No. 21272031) and the Fundamental Research Funds for the Central Universities (Grant No. wd01190).

Competing interests

The authors declare that they have no competing interests

Availabilityofdataandmaterials

The datasets used and analyzed during the current study are available from the corresponding author on reasonable request.

Code availability

Not applicable

Authors' contributions

Ruochen Fan: Formal analysis, Writing - original draft, conducted experiments, acquired data, analyzed data and wrote the paper. Zhuting Li: conducted experiments and acquired data. Xian Shi: conducted experiments and acquired data. Lulu Wang: conducted experiments and acquired data. Xuqiang Zhang: conducted experiments and acquired data. Chunshan Quan: Funding acquisition. Yuesheng Dong: Funding acquisition.

Ethics approval and consent to participate

Not applicable

Consent for publication

Not applicable

References

1. 1. Liu Y, Baba Y, Ishimoto T, Iwatsuki M, Hiyoshi Y, Miyamoto Y, et al. Progress in characterizing the linkage between Fusobacterium nucleatum and gastrointestinal cancer. Journal of gastroenterology. 2019;54(1):33–41.
2. 2. Luo K, Zhang Y, Xv C, Ji J, Lou G, Guo X, et al. Fusobacterium nucleatum, the communication with colorectal cancer. Biomedicine & Pharmacotherapy. 2019;116:108988.
3. 3. Bronzato JD, Bomfim RA, Edwards DH, Crouch D, Hector MP, Gomes BP. Detection of Fusobacterium in oral and head and neck cancer samples: A systematic review and meta-analysis. Archives of oral biology. 2020;112:104669.
4. 4. Wang X, Buhimschi CS, Temoin S, Bhandari V, Han YW, Buhimschi IA. Comparative microbial analysis of paired amniotic fluid and cord blood from pregnancies complicated by preterm birth and early-onset neonatal sepsis. PloS one. 2013;8(2):e56131.
5. 5. Weiss E, Shaniztki B, Dotan M, Ganeshkumar N, Kolenbrander P, Metzger Z. Attachment of Fusobacterium nucleatum PK1594 to mammalian cells and its coaggregation with periodontopathogenic bacteria are mediated by the same galactose-binding adhesin. Oral microbiology and immunology. 2000;15(6):371-7.
6. 6. Han YW, Redline RW, Li M, Yin L, Hill GB, McCormick TS. Fusobacterium nucleatum induces premature and term stillbirths in pregnant mice: implication of oral bacteria in preterm birth. Infection and immunity. 2004;72(4):2272-9.
7. 7. Kostic AD, Chun E, Robertson L, Glickman JN, Gallini CA, Michaud M, et al. Fusobacterium nucleatum potentiates intestinal tumorigenesis and modulates the tumor-immune microenvironment. Cell host & microbe. 2013;14(2):207 – 15.
8. 8. Yang Y, Weng W, Peng J, Hong L, Yang L, Toiyama Y, Gao R, Liu M, Yin M, Pan C, Li H, Guo B, Zhu Q, Wei Q, Moyer MP, Wang P, Cai S, Goel A, Qin H, Ma Y. Fusobacterium nucleatum Increases Proliferation of Colorectal Cancer Cells and Tumor Development in Mice by Activating Toll-Like Receptor 4 Signaling to Nuclear Factor-κB, and Up-regulating Expression of MicroRNA-21. Gastroenterology. 2017 Mar;152(4):851–866.e24.
9. 9. Wu J, Li K, Peng W, Li H, Li Q, Wang X, et al. Autoinducer-2 of Fusobacterium nucleatum promotes macrophage M1 polarization via TNFSF9/IL-1β signaling. International immunopharmacology. 2019;74:105724.
10. 10. Yu T, Guo F, Yu Y, Sun T, Ma D, Han J, Qian Y, Kryczek I, Sun D, Nagarsheth N, Chen Y, Chen H, Hong J, Zou W, Fang JY. Fusobacterium nucleatum Promotes Chemoresistance to Colorectal Cancer by Modulating Autophagy. Cell. 2017 Jul 27;170(3):548–563.e16.
11. 11. Kolenbrander PE, Palmer RJ, Periasamy S, Jakubovics NS. Oral multispecies biofilm development and the key role of cell–cell distance. Nature Reviews Microbiology. 2010;8(7):471 – 80.
12. 12. Han YW, Shi W, Huang GT-J, Haake SK, Park N-H, Kuramitsu H, et al. Interactions between periodontal bacteria and human oral epithelial cells: Fusobacterium nucleatum adheres to and

invades epithelial cells. Infection and immunity. 2000;68(6):3140-6.

13. 13. Alvarez AF, Barba-Ostria C, Silva-Jiménez H, Georgellis D. Organization and mode of action of two component system signaling circuits from the various kingdoms of life. Environmental microbiology. 2016;18(10):3210-26.
14. 14. Tierney AR, Rather PN. Roles of two-component regulatory systems in antibiotic resistance. Future microbiology. 2019;14(6):533 – 52.
15. 15. Mattos-Graner RO, Duncan MJ. Two-component signal transduction systems in oral bacteria. Journal of oral microbiology. 2017;9(1):1400858.
16. 16. Li X, Lv X, Lin Y, Zhen J, Ruan C, Duan W, et al. Role of two-component regulatory systems in intracellular survival of Mycobacterium tuberculosis. Journal of cellular biochemistry. 2019;120(8):12197-207.
17. 17. Zschiedrich CP, Keidel V, Szurmant H. Molecular mechanisms of two-component signal transduction. Journal of molecular biology. 2016;428(19):3752-75.
18. 18. Jacob-Dubuisson F, Mechaly A, Betton J-M, Antoine R. Structural insights into the signalling mechanisms of two-component systems. Nature Reviews Microbiology. 2018;16(10):585 – 93.
19. 19. Sidote DJ, Barbieri CM, Wu T, Stock AM. Structure of the Staphylococcus aureus AgrA LytTR domain bound to DNA reveals a beta fold with an unusual mode of binding. Structure. 2008;16(5):727 – 35.
20. 20. Sun F, Li C, Jeong D, Sohn C, He C, Bae T. In the Staphylococcus aureus two-component system sae, the response regulator SaeR binds to a direct repeat sequence and DNA binding requires phosphorylation by the sensor kinase SaeS. Journal of bacteriology. 2010;192(8):2111-27.
21. 21. Fan R, Shi X, Guo B, Zhao J, Liu J, Quan C, et al. The effects of L-arginine on protein stability and DNA binding ability of SaeR, a transcription factor in Staphylococcus aureus. Protein Expression and Purification. 2021;177:105765.
22. 22. Rooks MG, Veiga P, Reeves AZ, Lavoie S, Yasuda K, Asano Y, et al. QseC inhibition as an antivirulence approach for colitis-associated bacteria. Proceedings of the National Academy of Sciences. 2017;114(1):142-7.
23. 23. Massmig M, Reijerse E, Krausze J, Laurich C, Lubitz W, Jahn D, et al. Carnitine metabolism in the human gut: characterization of the two-component carnitine monooxygenase CntAB from Acinetobacter baumannii. Journal of Biological Chemistry. 2020;295(37):13065-78.
24. 24. Chen J, Ma M, Uzal FA, McClane BA. Host cell-induced signaling causes Clostridium perfringens to upregulate production of toxins important for intestinal infections. Gut Microbes. 2014;5(1):96–107.
25. 25. Goto R, Miki T, Nakamura N, Fujimoto M, Okada N. Salmonella Typhimurium PagP-and UgtL-dependent resistance to antimicrobial peptides contributes to the gut colonization. PloS one. 2017;12(12):e0190095.
26. 26. Wakimoto S, Nakayama-Imaohji H, Ichimura M, Morita H, Hirakawa H, Hayashi T, et al. PhoB regulates the survival of Bacteroides fragilis in peritoneal abscesses. PloS one. 2013;8(1):e53829.

27. 27. van der Stel AX, van Mourik A, Heijmen-van Dijk L, Parker CT, Kelly DJ, van de Lest CH, et al. The C ampylobacter jejuni RacRS system regulates fumarate utilization in a low oxygen environment. Environmental microbiology. 2015;17(4):1049-64.
28. 28. Giannakopoulou N, Mendis N, Zhu L, Gruenheid S, Faucher SP, Le Moual H. The virulence effect of CpxRA in Citrobacter rodentium is independent of the auxiliary proteins NlpE and CpxP. Frontiers in cellular and infection microbiology. 2018;8:320.
29. 29. Pacheco AR, Curtis MM, Ritchie JM, Munera D, Waldor MK, Moreira CG, et al. Fucose sensing regulates bacterial intestinal colonization. Nature. 2012;492(7427):113-7.
30. 30. Fujimoto M, Goto R, Haneda T, Okada N, Miki T. Salmonella enterica serovar Typhimurium CpxRA two-component system contributes to gut colonization in salmonella-induced colitis. Infection and immunity. 2018;86(7).
31. 31. Liu M, Hao G, Li Z, Zhou Y, Garcia-Sillas R, Li J, Wang H, Kan B, Zhu J. CitAB Two-Component System-Regulated Citrate Utilization Contributes to Vibrio cholerae Competitiveness with the Gut Microbiota. Infect Immun. 2019 Feb 21;87(3):e00746-18.
32. 32. Sonnenburg ED, Sonnenburg JL, Manchester JK, Hansen EE, Chiang HC, Gordon JI. A hybrid two-component system protein of a prominent human gut symbiont couples glycan sensing in vivo to carbohydrate metabolism. Proceedings of the National Academy of Sciences. 2006;103(23):8834-9.
33. 33. Lowe EC, Baslé A, Czjzek M, Firbank SJ, Bolam DN. A scissor blade-like closing mechanism implicated in transmembrane signaling in a Bacteroides hybrid two-component system. Proceedings of the National Academy of Sciences. 2012;109(19):7298 – 303.
34. 34. Hirakawa H, Kurushima J, Hashimoto Y, Tomita H. Progress Overview of Bacterial Two-Component Regulatory Systems as Potential Targets for Antimicrobial Chemotherapy. Antibiotics (Basel). 2020 Sep 23;9(10):635.
35. 35. Rosales-Hurtado M, Meffre P, Szurmant H, Benfodda Z. Synthesis of histidine kinase inhibitors and their biological properties. Medicinal research reviews. 2020;40(4):1440-95.
36. 36. Gumerov VM, Ortega DR, Adebali O, Ulrich LE, Zhulin IB. MiST 3.0: an updated microbial signal transduction database with an emphasis on chemosensory systems. Nucleic acids research. 2020;48(D1):D459-D64.
37. 37. Robert X, Gouet P. Deciphering key features in protein structures with the new ENDscript server. Nucleic acids research. 2014;42(W1):W320-W4.
38. 38. Letunic I, Khedkar S, Bork P. SMART: recent updates, new developments and status in 2020. Nucleic Acids Research. 2021;49(D1):D458-D60.
39. 39. Kelley LA, Mezulis S, Yates CM, Wass MN, Sternberg MJ. The Phyre2 web portal for protein modeling, prediction and analysis. Nature protocols. 2015;10(6):845 – 58.
40. 40. Unger T, Jacobovitch Y, Dantes A, Bernheim R, Peleg Y. Applications of the Restriction Free (RF) cloning procedure for molecular manipulations and protein expression. J Struct Biol. 2010 Oct;172(1):34–44.

41. 41. Zhang C, Li A, Wang R, Cao Y, Jiang H, Ouyang S, et al. Recombinant expression, purification and bioactivity characterization of extracellular domain of human tumor necrosis factor receptor 1. Protein expression and purification. 2019;155:21 – 6.
42. 42. Mueller AM, Breitsprecher D, Duhr S, Baaske P, Schubert T, Längst G. Microscale thermophoresis: a rapid and precise method to quantify protein–nucleic acid interactions in solution. Methods Mol Biol. 2017;1654:151–164.
43. 43. Walker JN, Crosby HA, Spaulding AR, Salgado-Pabón W, Malone CL, Rosenthal CB, et al. The Staphylococcus aureus ArlRS two-component system is a novel regulator of agglutination and pathogenesis. PLoS Pathog. 2013;9(12):e1003819.
44. 44. Fournier B, Hooper DC. A new two-component regulatory system involved in adhesion, autolysis, and extracellular proteolytic activity ofStaphylococcus aureus. Journal of bacteriology. 2000;182(14):3955-64.
45. 45. Nguyen M-P, Yoon J-M, Cho M-H, Lee S-W. Prokaryotic 2-component systems and the OmpR/PhoB superfamily. Canadian journal of microbiology. 2015;61(11):799–810.
46. 46. Bai J, Zhu X, Zhao K, Yan Y, Xu T, Wang J, et al. The role of ArlRS in regulating oxacillin susceptibility in methicillin-resistant Staphylococcus aureus indicates it is a potential target for antimicrobial resistance breakers. Emerging microbes & infections. 2019;8(1):503 – 15.
47. 47. Radin JN, Kelliher JL, Párraga Solórzano PK, Kehl-Fie TE. The two-component system ArlRS and alterations in metabolism enable Staphylococcus aureus to resist calprotectin-induced manganese starvation. PLoS pathogens. 2016;12(11):e1006040.
48. 48. Hayat SM, Farahani N, Golichenari B, Sahebkar A. Recombinant protein expression in Escherichia coli (E. coli): what we need to know. Current pharmaceutical design. 2018;24(6):718 – 25.
49. 49. Casali N. Escherichia coli host strains. Methods Mol Biol. 2003;235:27–48.
50. 50. Kapatral V, Anderson I, Ivanova N, Reznik G, Los T, Lykidis A, et al. Genome sequence and analysis of the oral bacterium Fusobacterium nucleatum strain ATCC 25586. Journal of bacteriology. 2002;184(7):2005-18.

Tables

Due to technical limitations, table 1 is only available as a download in the Supplemental Files section.

Figures

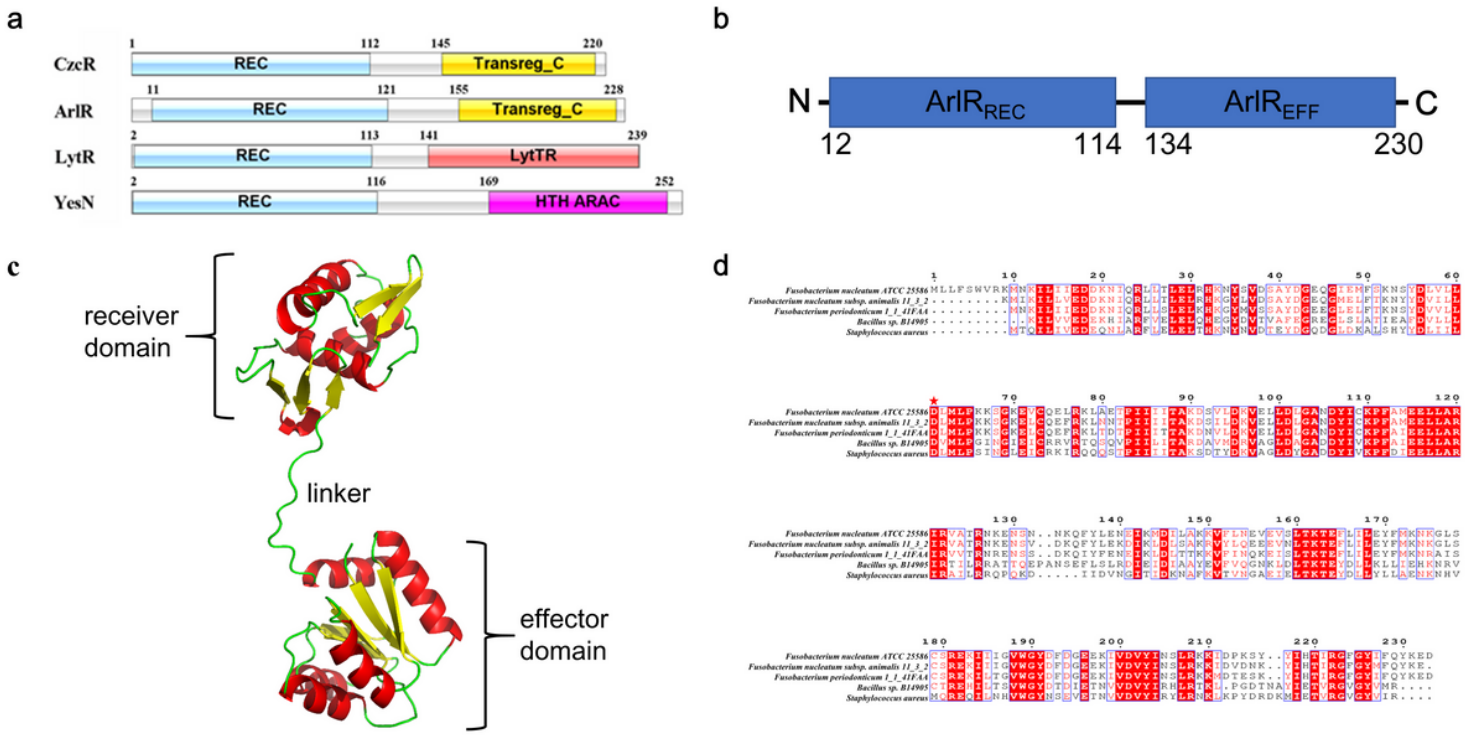

Figure 1

The molecular architecture of the two-component system response regulator protein and sequence alignment of ArlR protein in Fusobacterium nucleatum strain ATCC 25586 with ArlR in other strains. (a) The molecular architecture of the two-component system response regulator protein in Fusobacterium nucleatum ATCC 25586 predicted from SMART. REC: receiver domain; Transreg_C: transcriptional regulatory protein C-terminal; LytTR: LytTr DNA-binding domain; HTH_ARAC: helix-turn-helix arabinose operon control protein. (b) The molecular architecture of ArlR response regulator protein in Fusobacterium nucleatum strain ATCC 25586 predicted from Pfam. ArlRREC: ArlR receiver domain (from 12 to114th amino acid); ArlREFF: ArlR effector domain (from 134 to 230th amino acid). (c) The structure of ArlR response regulator protein in Fusobacterium nucleatum strain ATCC 25586 predicted from Phyre2. (d) Sequence alignment of ArlR protein in Fusobacterium nucleatum ATCC 25586 with ArlR protein in other strains. The conserved aspartic acid marked with a red asterisk is the predicted site receiving a phosphate group.

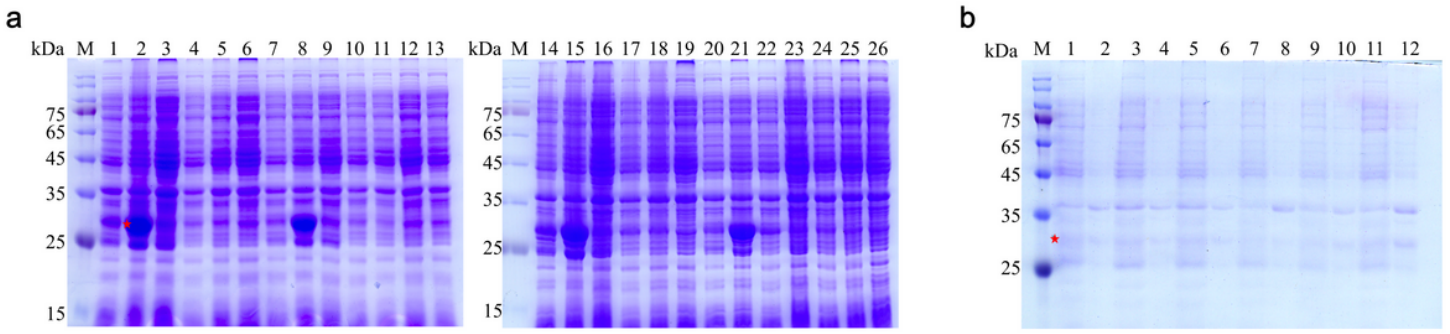

Figure 2

Optimizing of ArlR protein expression and purification conditions. (a) Screening of ArlR expression conditions in different host cells, culture temperature, and culture time: M-maker; 1. Transetta, 25 °C, 8 h; 2. RIL, 25 °C, 8 h; 3. pLysS, 25 °C, 8 h; 4. BL21, 25 °C, 8 h; 5. Tuner, 25 °C, 8 h; 6. C43, 25 °C, 8 h; 7. Transetta, 16 °C, 8 h; 8. RIL, 16 °C, 8 h; 9. pLysS, 16 °C, 8 h; 10. BL21, 16 °C, 8 h; 11. Tuner, 16 °C, 8 h; 12. C43, 16 °C, 8 h; 13. Control (BL21, 25 °C, 8 h, not induced); 14. Transetta, 25 °C, 20 h; 15. RIL, 25 °C, 20 h; 16. pLysS, 25 °C, 20 h; 17. BL21, 25 °C, 20 h; 18. Tuner, 25 °C, 20 h; 19. C43, 25 °C, 20 h; 20. Transetta, 16 °C, 20 h; 21. RIL, 16 °C, 20 h; 22. pLysS, 16 °C, 20 h; 23. BL21, 16 °C, 20 h; 24. Tuner, 16 °C, 20 h; 25. C43, 16 °C, 20 h; 26. Control (BL21, 25 °C, 20 h, not induced). The best expression conditions for ArlR are marked by a red asterisk. (b) Optimizing of ArlR purification conditions in buffers with different additives: M-maker; 1–2. 20 mM Tris-HCl, 150 mM NaCl, 5% glycerol; 3–4. 20 mM Tris-HCl, 150 mM NaCl, 50 mM L-Arg; 5–6. 20 mM Tris-HCl, 150 mM NaCl, 1% Triton X-100; 7–8. 20 mM Tris-HCl, 150 mM NaCl, 50 mM betaine; 9–10. 20 mM Tris-HCl, 150 mM NaCl, 50 mM L-Arg and 50 mM L-Glu; 11–12. 20 mM Tris-HCl, 150 mM NaCl; 1,3,5,7,9,11. Supernatant protein obtained after ultrasonication and centrifugation; 2, 4, 6, 8, 10, 12. Precipitate protein obtained after ultrasonication and centrifugation. The best purification conditions for ArlR are marked by a red asterisk.

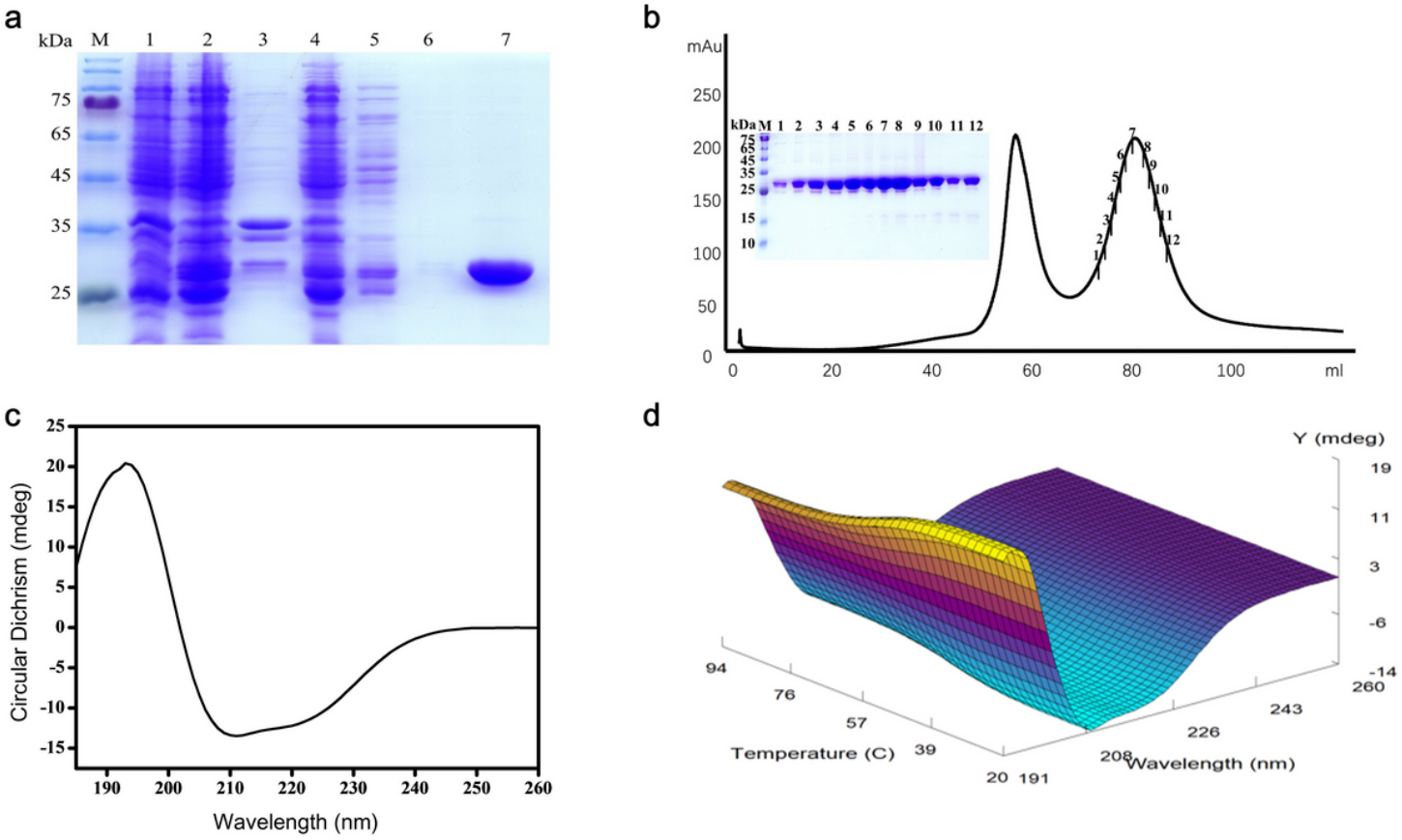

Figure 3

The secondary structure and thermal stability of the purified ArlR protein. (a) SDS-PAGE analysis of the expression and purification of ArlR: M-maker; 1. Protein after ultrasonication; 2. Supernatant protein after ultrasonication and centrifugation; 3. Precipitant protein after ultrasonication and centrifugation; 4.

Unbound protein on nickel column; 5–6. Washing buffer eluted protein; 7. Elution buffer eluted protein (b) SDS-PAGE analysis of the ArlR purified by gel filtration chromatography. M: maker; the numbers 1–12 correspond to the fractions on the chromatogram. (c) The circular dichroism spectrum of the purified ArlR protein. (d) Circular dichroism spectrum of purified ArlR at varying temperatures from 20 °C to 94 °C.

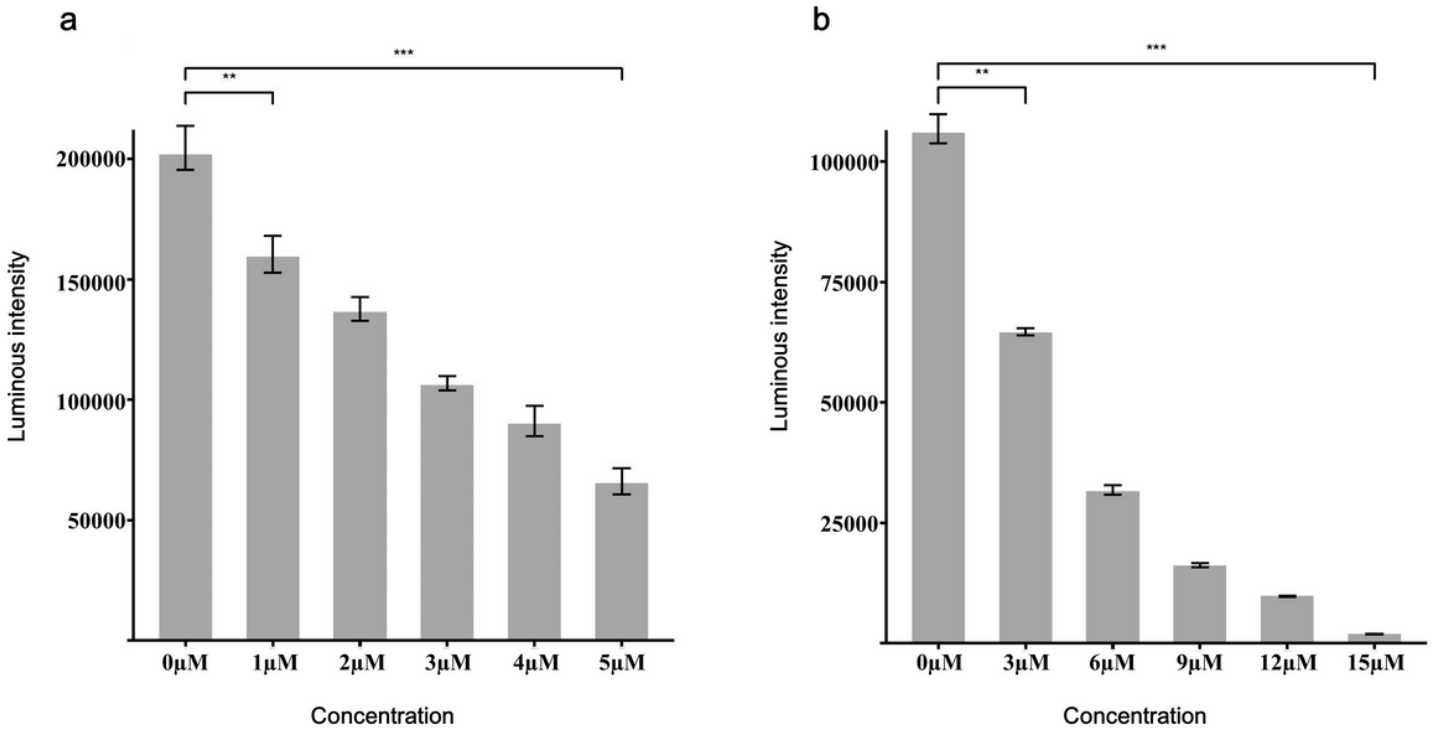

Figure 4

The kinase activity of ArlSC and the phosphotransferase activity of P-ArlSC to ArlR. ATP as a substrate by the Ultra-Glo™ Luciferase to catalyze producing photon of light. Hence, Luminescence intensity is directly proportional to the amount of ATP persisting in the reaction solution and inversely proportional to histidine-kinase activity or phosphotransferase activity. (a) The luminescence intensity of kinase reaction buffer. As the ArlSC protein concentration gradually increases, the luminescence intensity of the buffer gradually decreases, i.e., the remaining ATP content in the reaction solution gradually decreases, indicating that the ArlSC protein can bind ATP and has histidine-kinase activity. (b) The luminescence intensity of phosphotransferase reaction buffer. As the ArlR protein concentration gradually increases, the luminescence intensity gradually decreases, i.e., the remaining ATP content in the reaction solution gradually decreases, indicating that the P-ArlSC protein can transfer phosphate group to ArlR. The experiment was repeated three times. Error bars represent average difference between the data points and their mean. **, $p < 0.01$, ***, $p < 0.001$.

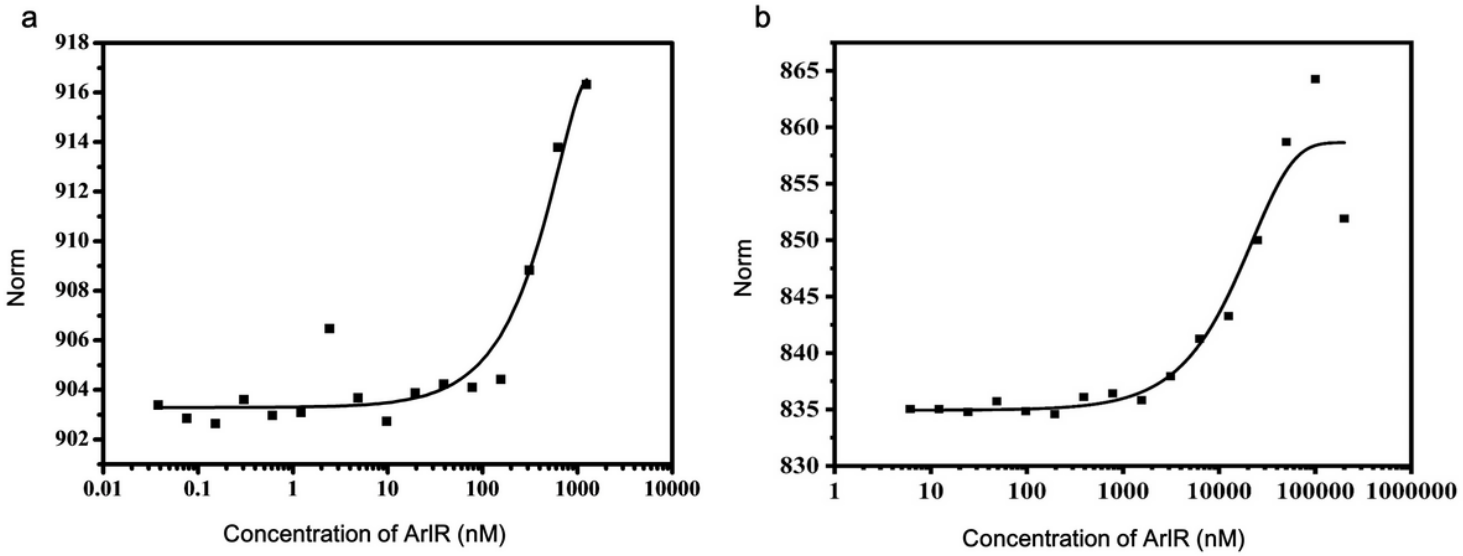

Figure 5

The interaction between P-ArlSC and its corresponding response regulator protein ArlR, and binding of P-ArlR to its promoter measured by MST assay. (a) MST showing the interaction between P-ArlSC and ArlR with Kd= 1.28 μM. (b) MST showing the binding of P-ArlR to its own promoter with Kd= 37.5 μM.

Supplementary Files

This is a list of supplementary files associated with this preprint. Click to download.

- Table1.tiff.tif